

Supplementary Information

Synthesis and coordination behavior of Cu^I bis(phosphaethenyl)pyridine complexes

Yumiko Nakajima,^{a,b} Yu Shiraishi,^b Takahiro Tsuchimoto^b and Fumiyuki Ozawa^{a,b}

^a International Research Center for Elements Science (IRCELS), Institute for Chemical Research, Kyoto University, Uji, Kyoto 611-0011, Japan.

^b Department of Energy and Hydrocarbon Chemistry, Graduate School of Engineering, Kyoto University, Uji, Kyoto 611-0011, Japan.

E-mail: nakajima@scl.kyoto-u.ac.jp, ozawa@scl.kyoto-u.ac.jp

Contents

Experimental Section

- Table S1** Crystallographic data for **1**, **2a**, **3**, **4**, **6**, **7a**
Fig. S1 ORTEP drawing of **1** with 50% probability ellipsoids
Table S2 Selected bond lengths (Å) and angles (deg) for **1**
Fig. S2 ORTEP drawing of **2a** with 50% probability ellipsoids
Table S3 Selected bond lengths (Å) and angles (deg) for **2a**
Fig. S3 ORTEP drawing of **3** with 50% probability ellipsoids
Table S4 Selected bond lengths (Å) and angles (deg) for **3**
Fig. S4 ORTEP drawing of **4** with 50% probability ellipsoids
Table S5 Selected bond lengths (Å) and angles (deg) for **4**
Fig. S5 ORTEP drawing of **6** with 50% probability ellipsoids
Table S6 Selected bond lengths (Å) and angles (deg) for **6**
Fig. S6 ORTEP drawing of **7a** with 50% probability ellipsoids

Computational Details

- Fig. S 7** Optimized geometry of **6'** (a) and **6'^{FREE}** (b)
Table S7 Selected bond lengths and angles of **6'** and **6'^{FREE}**
Table S8 Absolute total energies (in Hartree) of **6'** and **6'^{FREE}**
Table S9 Natural charge by NBO analysis
Table S10 Mayer's bond order
Fig. S8 Imaginary frequency of **6'**
Fig. S9 Imaginary frequency of **6'^{FREE}** (−15.86 *i* cm^{−1})
Fig. S10 Selected Kohn-sham orbitals of **6'** including orbital overlaps between Cu and PF₆
Table S11 Cartesian coordinates of **6'**
Table S12 Cartesian coordinates of **6'^{FREE}**
Table S13 Cartesian coordinates of [Cu(BPEP)]⁺
Table S14 Cartesian coordinates of PF₆[−]

References

Experimental Section

General Considerations. All manipulations were performed under a dry and oxygen-free dinitrogen atmosphere using Schlenk techniques or a glove box. Solvents were dried over sodium/benzophenone ketyl (toluene, benzene, pentane, Et₂O) or CaH₂ (CH₂Cl₂) and distilled. CuBr (Wako), AgPF₆, AgSbF₆ (Strem), and Me₃SiN₃ (Sigma-Aldrich) were obtained from commercial sources and used without purification. BPEP was prepared according to the literature method.¹

¹H NMR spectra were recorded on a Bruker AVANCHE 400 spectrometer (¹H NMR, 400.13 MHz; ¹³C NMR, 100.62 MHz; ¹⁹F NMR, 376.46 MHz; ³¹P NMR, 161.98 MHz). Chemical shifts are reported in δ (ppm), referenced to ¹H (residual) and ¹³C signals of deuterated solvents as internal standards or to the ¹⁹F signal of C₆F₆ (δ -163.0) and the ³¹P signal of 85% H₃PO₄ (δ 0.0) as external standards. Elemental analysis was performed by the ICR Analytical Laboratory, Kyoto University. IR spectra were recorded on a JASCO FT/IR-410 spectrometer.

Preparation of [CuBr(BPEP)] (1). A mixture of CuBr (35.6 mg, 24.7 μmol) and BPEP (200.2 mg, 24.8 μmol) in toluene (6 mL) was heated at 90 °C for 12 h. The solvent was removed under reduced pressure at room temperature. The residue was washed with hexane, dissolved in toluene, and filtered through a celite pad. The filtrate was concentrated to dryness to afford a dark green solid of **1**, which was analytically pure (232.2 mg, 24.4 μmol, 99%). ¹H NMR (C₆D₆, 20 °C): δ 1.32 (18H, s), 1.66 (36H, s), 6.81 (4H, m), 6.92 (4H, m), 7.01 (1H, t, *J* = 9.8 Hz), 7.27 (4H, d, *J* = 8.0 Hz), 7.48 (4H, s). ¹³C{¹H} NMR (C₆D₆, 20 °C): δ 31.7, 35.2, 35.5, 39.9, 123.2, 123.7, 126.0, 127.7, 129.7, 131.5, 134.3, 139.6, 153.0, 156.7, 157.3, 167.9. ³¹P{¹H} NMR (20 °C): δ 251.5 (C₆D₆ and CD₂Cl₂). Anal. Found: C, 69.12; H, 7.61; N, 1.40. Calcd for C₅₅H₇₁BrCuNP₂: C, 69.42; H, 7.52; N, 1.47. Single crystals suitable for X-ray diffraction analysis were obtained by slow diffusion of pentane into a CH₂Cl₂ solution of **1**.

Preparation of [Cu(SbF₆)(BPEP)] (2a). A suspension of AgSbF₆ (78.4 mg, 0.228 mmol) in toluene (3 mL) was added to a solution of **1** (198.9 mg, 0.209 mmol) in toluene (3 mL) at -30 °C. The mixture was stirred at room temperature for a few minutes, and filtered through a celite pad to remove the precipitate of AgBr formed in the system. The filtrate was concentrated under reduced pressure to afford a dark red solid of **2a** (224.6 mg, 0.203 mmol, 97%). Single crystals suitable for X-ray diffraction analysis were obtained by allowing to stand the saturated toluene solution at room temperature for 8 days. ¹H NMR (CD₂Cl₂, 20 °C): δ 1.33 (18H, s), 1.57 (36H, s), 6.68 (4H, d, *J* = 6.8 Hz), 7.12 (4H, t, *J* = 7.6 Hz), 7.24 (4H, m), 7.39 (4H, s), 7.70 (1H, s). ¹³C{¹H} NMR (CD₂Cl₂, 20 °C): δ 31.5, 34.6, 35.6, 39.2, 123.7, 125.8, 128.4, 128.7, 129.5, 130.0, 137.0, 138.3, 153.7, 156.6, 157.1. The ¹³C NMR signal of P=C was obscure due to low signal intensity. ³¹P{¹H} NMR (CD₂Cl₂, 20 °C): δ 213.3 (br). IR (KBr, cm⁻¹): 655, 461 (ν(SbF₆)). Anal. Found: C, 59.37; H, 6.60; N, 1.14. Calcd for C₅₅H₇₁CuF₆NP₂Sb: C, 59.65; H, 6.46; N, 1.26.

Preparation of [Cu(PF₆)(BPEP)] (2b). Complex **2b** was similarly prepared from **1** (19.5 mg, 2.1 μmol) and AgPF₆ (4.8 mg, 2.2 μmol) in 71% yield (15.0 mg, 1.5 μmol). Because a part of **2b** was converted to **6** in the concentrated solution during isolation, elementary analysis was not performed. The ¹H and ¹³C NMR data in CD₂Cl₂ were identical to those of **2a**. ³¹P{¹H} NMR (CD₂Cl₂, 20 °C): δ -143.9 (sep, ¹*J*_{PF} = 711 Hz, PF₆⁻), 213.3 (br). ¹⁹F NMR (CD₂Cl₂, 20 °C): δ -73.55 (d, ¹*J*_{PF} = 711 Hz, PF₆⁻). IR (KBr, cm⁻¹): 844, 607 (ν(PF₆⁻)).

Preparation of [Cu(MeCN)(BPEP)]⁺SbF₆⁻ (3). Complex **2a** (10.8 mg, 9.8 μmol), freshly prepared from **1** and AgSbF₆ in toluene, was dissolved in CD₂Cl₂ (0.4 mL) in an NMR sample tube, and MeCN (0.5 μL, 19.5 μmol) was added. ¹H NMR analysis revealed quantitative formation of **3**. The solution was concentrated under reduced pressure, layered with hexane, and allowed to stand at room temperature to afford red crystals of **3**, containing toluene as a crystal solvent (6.3 mg, 5.5 μmol, 56%). The NMR data for the cationic part are as follows. ¹H NMR (CD₂Cl₂, 20 °C): δ 1.35 (18H, s), 1.47 (36H, s), 2.26 (3H, s), 6.65 (4H, d, *J* = 7.6 Hz), 7.10 (4H, t, *J* = 8.0 Hz), 7.17–7.26 (4H, m), 7.36 (4H, s), 7.63 (1H, t, *J* = 8.0 Hz). ¹³C{¹H} NMR (CD₂Cl₂, 20 °C): δ 1.5 (CH₃CN), 31.6, 34.6, 35.7, 39.2, 121.2 (CH₃CN), 123.6, 123.8, 126.2, 128.5, 128.7, 129.7, 138.1, 138.7, 154.3, 156.9, 157.2, 176.6. ³¹P{¹H} NMR (CD₂Cl₂, 20 °C): δ 251.1 (br). Anal. Found: C, 61.80; H, 6.77; N, 2.32. Calcd for C₅₇H₇₄CuF₆N₂P₂Sb•0.5C₇H₈: C, 60.81; H, 6.58; N, 2.35.

Preparation of [Cu(CO)(BPEP)]⁺SbF₆⁻ (4). Complex **2a** (17.8 mg, 16.1 μmol) was dissolved in CH₂Cl₂ (1 mL), and degassed at –196 °C. Atmospheric pressure of CO was introduced from a balloon. The color of the solution immediately turned light orange. Hexane (ca. 1 mL) was slowly layered, and the mixture was allowed to stand at –5 °C overnight, giving orange crystals of **4**, which contains CH₂Cl₂ as a crystal solvent (5.49 mg, 4.8 μmol, 30%). The NMR data for the cationic part are as follows. ¹H NMR (CD₂Cl₂, 20 °C): δ 1.34 (18H, s), 1.55 (36H, s), 6.72 (4H, d, *J* = 7.6 Hz), 7.12 (4H, t, *J* = 8.0 Hz), 7.22–7.28 (4H, m), 7.39 (4H, s), 7.71 (1H, t, *J* = 8.0 Hz). ¹³C{¹H} NMR (CD₂Cl₂, 20 °C): δ 31.5, 34.7, 35.7, 39.2, 123.9, 124.0, 124.8, 128.7, 129.3, 129.5, 137.2, 140.1, 155.1, 157.4, 157.9, 178.5. The ¹³C NMR signal of CO was obscure due to quadrupole couplings with Cu. ³¹P{¹H} NMR (CD₂Cl₂, 20 °C): δ 227.3 (br). IR (KBr, cm⁻¹): 2131 (ν(CO)). Anal. Found: C, 55.68; H, 6.02; N, 1.16. Calcd for C₅₆H₇₁CuF₆NOP₂Sb•CH₂Cl₂: C, 56.08; H, 6.03; N, 1.15.

Preparation of [Cu(^tBuNC)(BPEP)]⁺SbF₆⁻ (5). Complex **2a** (10.3 mg, 9.3 μmol) was dissolved in CD₂Cl₂ (0.6 mL), and ^tBuNC (1.1 μL, 9.9 μmol) was added at room temperature. The color of the solution immediately turned light red, and the NMR spectroscopy showed complete conversion of **2a** to **5**. All the volatiles were removed under vacuum, and the residue was washed with hexane and dried (10.2 mg, 8.6 μmol, 92%). ¹H NMR (CD₂Cl₂, 20 °C): δ 1.34 (18H, s), 1.47 (36H, s), 1.49 (9H, s, ^tBuNC), 6.61 (4H, brs), 7.07, 7.17, 7.30, 7.35 (totally 12H, brs), 7.67 (1H, brs). ¹³C{¹H} NMR (CD₂Cl₂, 20 °C): δ 29.9 (^tBuNC), 30.9, 34.2, 35.0, 38.6, 58.7 (^tBuNC), 123.1, 123.3, 126.0, 127.9, 128.1, 129.3, 137.2, 137.6, 153.9, 156.2, 156.9, 174.8. The ¹³C NMR signal of ^tBuNC was obscure due to quadrupole couplings with Cu. ³¹P{¹H} NMR (CD₂Cl₂, 20 °C): δ 261.5 (br). IR (KBr, cm⁻¹): 2198 (ν(CN)). Anal. Found: C, 60.61; H, 6.81; N, 2.39. Calcd for C₆₀H₈₀CuF₆NP₂Sb: C, 60.53; H, 6.77; N, 2.35.

Preparation of [Cu₂(μ-PF₆)(BPEP)₂]⁺PF₆⁻ (6). A solution **2b** (16.4 mg, 16.1 μmol) in toluene (1 mL) was allowed to stand at room temperature for 2 days, to afford dark red crystals of **6**, which was washed with toluene and dried under vacuum (10.1 mg, 0.00497 mmol, 62%). ¹H NMR (CD₂Cl₂, 20 °C): δ 1.32 (36H, s), 1.45 (72H, s), 6.67 (8H, d, *J* = 7.6 Hz), 7.08 (8H, t, *J* = 8.0 Hz), 7.20 (8H, m), 7.35 (8H, s), 7.61 (2H, t, *J* = 7.6 Hz). ¹³C{¹H} NMR (CD₂Cl₂, 20 °C): δ 30.9, 34.0, 35.0, 38.6, 123.2, 123.7, 124.9, 127.9, 128.3, 129.1, 137.4, 137.6, 153.5, 156.2 (2C), 175.5. ³¹P{¹H} NMR (CD₂Cl₂, 20 °C): δ –143.9 (sep, ¹*J*_{PF} = 711 Hz, PF₆⁻), –17.3 (t, ¹*J*_{PF} = 978 Hz, μ-PF₆), 244.7 (br, BPEP). ¹⁹F NMR (CD₂Cl₂, 20 °C): δ –77.8 (d, ¹*J*_{PF} = 978 Hz, μ-PF₆), –73.7 (d, ¹*J*_{PF} = 711 Hz, PF₆⁻). Anal. Found: C, 65.27; H, 7.04; N, 1.39. Calcd for C₁₁₀H₁₄₂Cu₂F₁₂N₂P₆: C, 64.98; H, 7.04; N, 1.38. IR (KBr,

cm^{-1}): 876 ($\nu(\mu\text{-PF}_6^-)$), 843 ($\nu(\text{PF}_6^-)$), 808 ($\nu(\mu\text{-PF}_6^-)$), 557 ($\nu(\text{PF}_6^-)$).

Reaction of 2a with Me_3SiN_3 to give $[\text{Cu}_2(\mu\text{-N}_3)(\text{BPEP})_2]^+\text{SbF}_6^-$ (7a**).** Complex **2a** (6.8 mg, 6.2 μmol) and mesitylene (1.3 mg, 11 μmol) as an internal standard were placed in an NMR sample tube, and dissolved in CD_2Cl_2 (0.6 mL) at room temperature. Me_3SiN_3 (0.9 mg, 7.8 μmol) was added, and the mixture was heated at 50 °C for 14 h. ^1H NMR analysis revealed the absence of **2a** and the formation of Me_3SiF (3.3 μmol). The mixture was concentrated to dryness, and the residue was washed with hexane and dried under vacuum to give a dark red solid of **7a** (6.2 mg, 3.0 μmol , 97%). The crude product was dissolved in toluene and allowed to stand at -30 °C to give single crystals suitable for X-ray diffraction analysis. ^1H NMR (CD_2Cl_2 , 20 °C): δ 1.33 (36H, s), 1.41 (72H, s), 6.61 (8H, d, $J = 7.2$ Hz), 7.07 (8H, t, $J = 8.0$ Hz), 7.15-7.24 (8H, m), 7.30 (8H, s), 7.60 (2H, t, $J = 8.0$ Hz). $^{13}\text{C}\{^1\text{H}\}$ NMR (CD_2Cl_2 , 20 °C): δ 31.5, 34.2, 35.6, 38.9, 123.2, 123.5, 128.2, 128.3, 129.5, 129.7, 137.6, 138.2, 153.8, 156.4, 156.9, 174.8. $^{31}\text{P}\{^1\text{H}\}$ NMR (CD_2Cl_2 , 20 °C): δ 255.7 (br). IR (KBr, cm^{-1}): 2130 ($\nu(\text{N}_3)$). Anal. Found: C, 65.04; H, 7.06; N, 3.57. Calcd for $\text{C}_{110}\text{H}_{142}\text{Cu}_2\text{F}_6\text{N}_5\text{P}_4\text{Sb}$: C, 65.37; H, 7.08; N, 3.47.

Reaction of 2b with Me_3SiN_3 to give $[\text{Cu}_2(\mu\text{-N}_3)(\text{BPEP})_2]^+\text{PF}_6^-$ (7b**).** Complex **2b** was freshly prepared from **1** (18.6 mg, 0.020 mmol) and AgPF_6 (5.5 mg, 0.022 mmol) in toluene. To a concentrated toluene solution of **2b**, Me_3SiN_3 (1.0 mg, 8.7 μmol) was added at room temperature. After the solution was heated at 50 °C for 2 h, the solvent was removed under vacuum. The residue was dissolved in toluene (0.2 mL) and allowed to stand at -30 °C to give **7b** (7.0 mg, 0.0036 mmol, 36%) as red crystals. The ^1H and ^{13}C data in CD_2Cl_2 were identical to those of **7a**. $^{31}\text{P}\{^1\text{H}\}$ NMR (CD_2Cl_2 , 20 °C): δ -143.9 (sep, $^1J_{\text{PF}} = 711$ Hz, PF_6^-), 255.7 (br, BPEP). ^{19}F NMR (CD_2Cl_2 , 20 °C): δ -73.80 (d, $^1J_{\text{PF}} = 711$ Hz, PF_6^-). IR (KBr, cm^{-1}): 2123 ($\nu(\text{N}_3)$). Anal. Found: C, 68.22; H, 7.51; N, 3.92. Calcd for $\text{C}_{110}\text{H}_{142}\text{Cu}_2\text{F}_6\text{N}_5\text{P}_3$: C, 68.45; H, 7.41; N, 3.63.

X-Ray crystal structure determination. The intensity data were collected on a Rigaku Mercury CCD diffractometer for **2a**, **3**, **4** and **7a**, and on a Rigaku VariMax diffractometer for **1** and **6** with graphite-monochromated Mo $K\alpha$ radiation ($\lambda = 0.71070$ Å). The frame data were integrated using the CrystalClear program package. The data sets were corrected for Lorentz and polarization effects and absorption. The structures were solved by direct method (SHELXS-97²) and refined on F^2 for all reflections (SHELXL-97).³ In the structure of **1**, two $t\text{Bu}$ groups and CH_2Cl_2 were disordered. In the structure of **2a**, one $t\text{Bu}$ group and one fluorine atom of the SbF_6^- unit were disordered. In the structure of **3**, three $t\text{Bu}$ groups were disordered. In the structure of **4**, two $t\text{Bu}$ groups, SbF_6^- and incorporated CH_2Cl_2 were disordered. In the structure of **6**, three $t\text{Bu}$ groups were disordered. Anisotropic refinement was applied to all non-hydrogen atoms except for disordered groups. Hydrogen atoms were placed at calculated positions. The structure of **7a** could not be fully characterized because of poor data sets, while the dinuclear structure was confirmed. The crystallographic data and the summary of solution and refinement are listed in Table S1. The molecular structures and selected structural data are given in Figures S1–S6 and Tables S2–S6. Further information has been deposited with the Cambridge Crystallographic Data Center. CCDC reference numbers: 812261 (**1**), 812262 (**2a**), 812263 (**3**), 812264 (**4**), 812265 (**6**).

Table S1 Crystallographic data for **1**, **2a**, **3**, **4**, **6**, and **7a**

Compound	1	2a	3	4	6	7a
Empirical formula	C ₅₅ H ₇₁ BrCuNP ₂ · 0.5CH ₂ Cl ₂	C ₅₅ H ₇₁ CuF ₆ NP ₂ Sb	C ₆₄ H ₈₂ CuF ₆ N ₂ P ₂ Sb · 0.5C ₇ H ₈	C ₅₇ H ₇₁ CuF ₆ NOSb · CH ₂ Cl ₂	C ₅₅ H ₇₁ CuF ₆ NP ₃	C ₁₁₀ H ₁₄₂ Cu ₂ F ₆ N ₅ P ₄ Sb
Fw	993.98	1107.36	1286.61	1220.29	1016.58	2021.00
Crystal system	Monoclinic	Monoclinic	Triclinic	Monoclinic	Triclinic	Triclinic
space group	<i>P</i> ₂ / <i>c</i>	<i>P</i> ₂ / <i>c</i>	<i>P</i> (-1)	<i>P</i> ₂ / <i>a</i>	<i>P</i> (-1)	<i>P</i> ₂ / <i>c</i>
<i>a</i> (Å)	15.9441(2)	11.715(2)	12.075(3)	18.330(7)	11.5918(16)	18.68(6)
<i>b</i> (Å)	9.64940(2)	24.683(5)	17.639(4)	18.284(6)	13.059(2)	19.13(3)
<i>c</i> (Å)	35.0720(7)	19.400(4)	17.853(4)	18.673(7)	19.304(3)	19.42(3)
<i>α</i> (deg)		90.00	111.242(3)	90.00	71.143(3)	103.09(6)
<i>β</i> (deg)	96.2821(8)	106.209(3)	101.392(2)	110.230(4)	73.149(8)	115.06(7)
<i>γ</i> (deg)		90.00	105.3822(15)	90.00	76.891(8)	109.46(6)
<i>V</i> (Å ³)	5363.46(14)	5386.7(18)	3229.7(13)	5872(3)	2618.0(7)	5352(19)
<i>Z</i>	4	4	2	4	2	2
<i>μ</i> (Mo <i>Kα</i>) (mm ⁻¹)	1.296	1.012	0.854	1.024	0.566	0.762
temp (K)	103(2)	173(2)	173(2)	173(2)	103(2)	173(2)
reflections collected	52478	51160	31379	47440	21606	51425
unique reflections	9450	16150	17862	13047	11509	29651
	(<i>R</i> _{int} = 0.0715)	(<i>R</i> _{int} = 0.0565)	(<i>R</i> _{int} = 0.0391)	(<i>R</i> _{int} = 0.0557)	(<i>R</i> _{int} = 0.0331)	(<i>R</i> _{int} = 0.1245)
GOF	1.232	1.396	1.137	1.991	1.284	1.315
final <i>R</i> indices	<i>R</i> ₁ = 0.0818	<i>R</i> ₁ = 0.0875	<i>R</i> ₁ = 0.0836	<i>R</i> ₁ = 0.1005	<i>R</i> ₁ = 0.0719	<i>R</i> ₁ = 0.1973
(<i>I</i> > 2σ(<i>I</i>))	<i>wR</i> ₂ = 0.1827	<i>wR</i> ₂ = 0.2267	<i>wR</i> ₂ = 0.1853	<i>wR</i> ₂ = 0.3153	<i>wR</i> ₂ = 0.1985	<i>wR</i> ₂ = 0.3534
<i>R</i> indices	<i>R</i> ₁ = 0.0969	<i>R</i> ₁ = 0.1036	<i>R</i> ₁ = 0.1073	<i>R</i> ₁ = 0.1099	<i>R</i> ₁ = 0.0848	<i>R</i> ₁ = 0.3180
(all data)	<i>wR</i> ₂ = 0.1902	<i>wR</i> ₂ = 0.2270	<i>wR</i> ₂ = 0.2025	<i>wR</i> ₂ = 0.3193	<i>wR</i> ₂ = 0.2095	<i>wR</i> ₂ = 0.4191

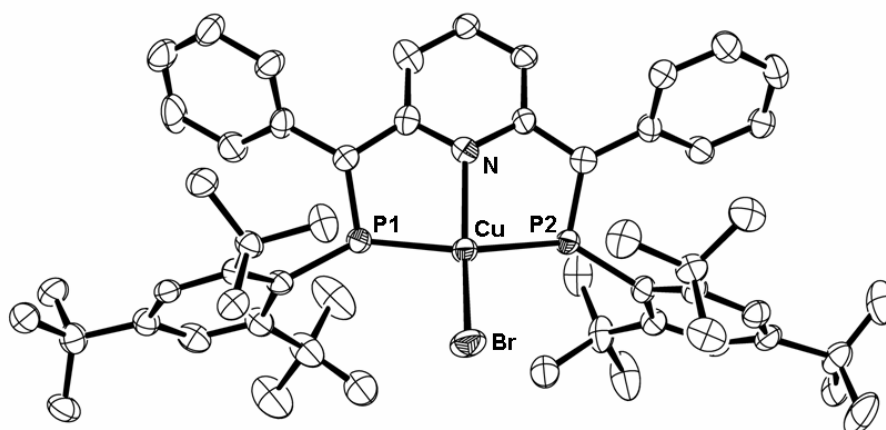


Fig. S1 ORTEP drawing of **1** with 50% probability ellipsoids. Hydrogen atoms, disordered *tert*-butyl groups, and an incorporated CH₂Cl₂ molecule were omitted for clarity.

Table S2 Selected bond lengths (Å) and angles (deg) for **1**

Cu-N	2.070(5)	N-Cu-Br	152.32(14)
Cu-P1	2.2390(19)	N-Cu-P1	82.34(15)
Cu-P2	2.2396(18)	N-Cu-P2	81.83(15)
Cu-Br	2.3381(11)	P1-Cu-P2	143.84(7)
		P1-Cu -Br	105.06(6)
		P2-Cu-Br	104.03(6)

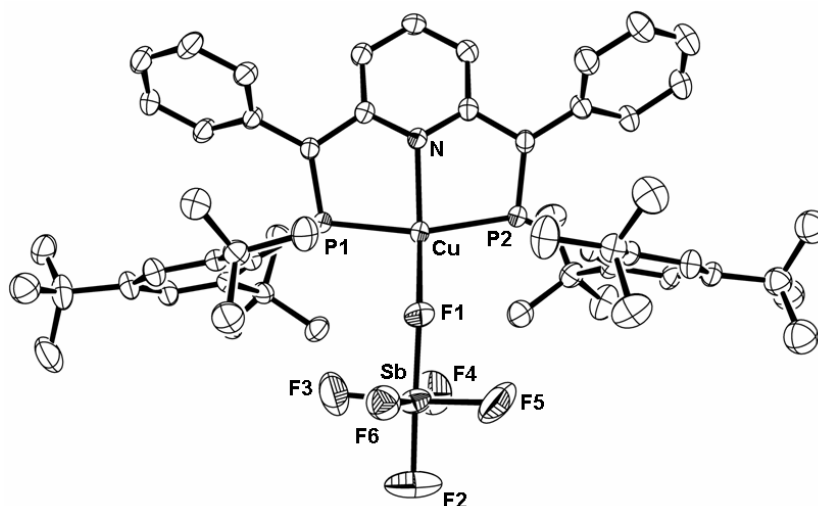


Fig. S2 ORTEP drawing of **2a** with 50% probability ellipsoids. Hydrogen atoms, disordered *tert*-butyl groups, and disordered F6 atom were omitted for clarity.

Table S3 Selected bond lengths (Å) and angles (deg) for **2a**

Cu-N	2.107(3)	N-Cu-F1	146.05(15)
Cu-P1	2.2526(11)	N-Cu-P1	82.98(9)
Cu-P2	2.2612(11)	N-Cu-P2	82.32(9)
Cu-F1	2.190(3)	P1-Cu-P2	156.25(5)
Sb-F1	1.916(3)	Cu-F1-Sb	143.9(2)
Sb-F2	1.843(4)	P1-Cu-F1	100.63(10)
Sb-F3	1.859(5)	P2-Cu-F2	101.99(10)
Sb-F4	1.846(4)		
Sb-F5	1.850(5)		

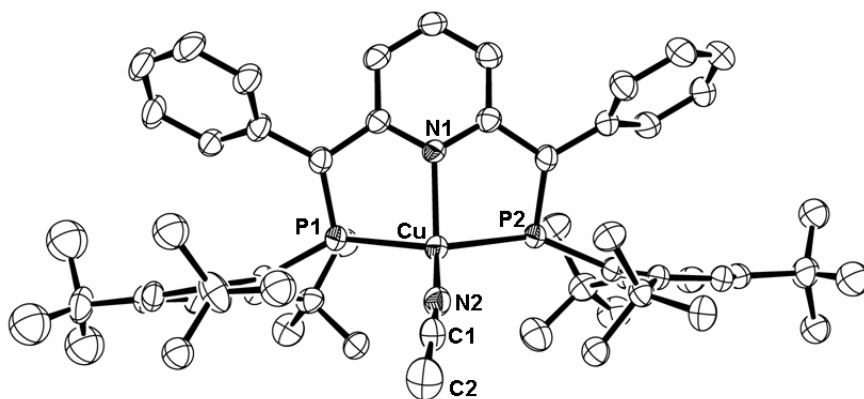


Fig. S3 ORTEP drawing of **3** with 50% probability ellipsoids. Hydrogen atoms, disordered *tert*-butyl groups, an incorporated toluene molecule, and a free SbF_6 anion were omitted for clarity.

Table S4 Selected bond lengths (Å) and angles (deg) for **3**

Cu-N1	2.059(3)	N1-Cu-N2	131.57(16)
Cu-P1	2.2828(12)	N2-Cu-P1	81.32(10)
Cu-P2	2.2900(12)	N2-Cu-P2	82.45(10)
Cu-N2	1.928(4)	P1-Cu-P2	137.65(5)
N2-C1	1.138(6)	Cu-N2-C1	174.8(4)
C1-C2	1.460(7)	N2-C1-C2	178.2(5)
		P1-Cu-N2	108.87(12)
		P2-Cu-N2	111.17(12)

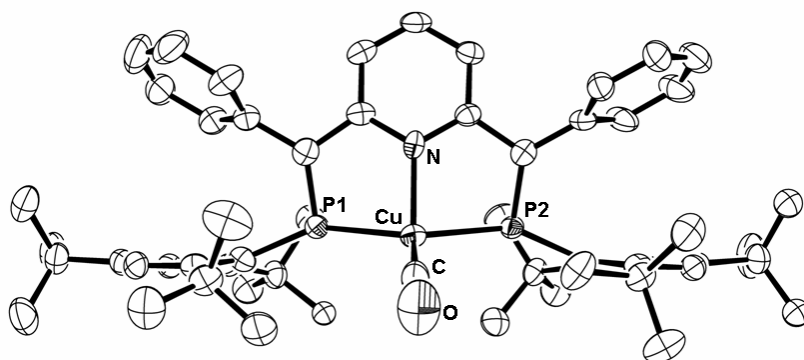


Fig. S4 ORTEP drawing of **4** with 50% probability ellipsoids. Hydrogen atoms, disordered *tert*-butyl groups, an incorporated CH_2Cl_2 molecule, and a free SbF_6 anion were omitted for clarity.

Table S5 Selected bond lengths (Å) and angles (deg) for **4**

Cu-N	2.007(6)	N-Cu-C	128.0(3)
Cu-P1	2.3164(18)	N-Cu-P1	81.96(15)
Cu-P2	2.3272(18)	N-Cu-P2	81.78(14)
Cu-C	1.857(9)	P1-Cu-P2	135.33(7)
C-O	1.121(11)	Cu-C-O	176.3(9)
		P1-Cu-C	113.9(2)
		P2-Cu-C	108.9(2)

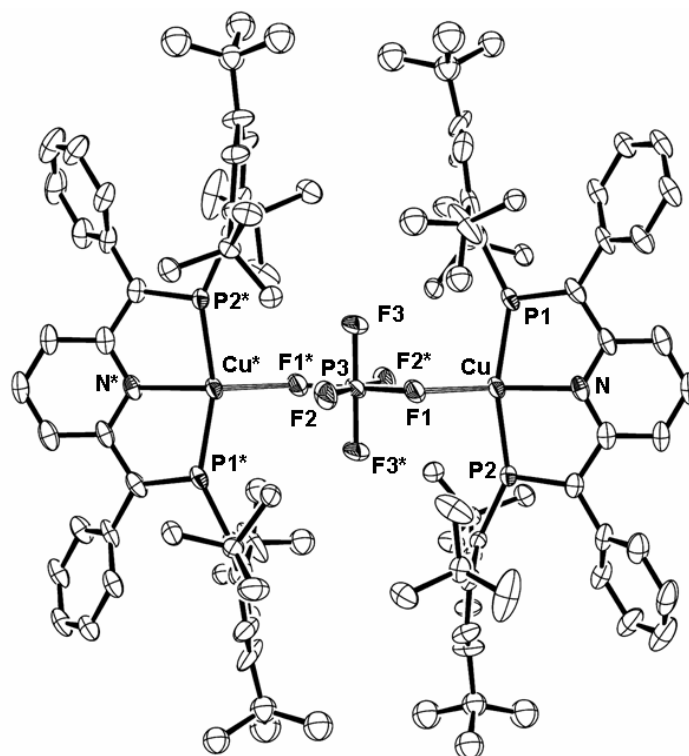


Fig. S5 ORTEP drawing of **6** with 50% probability ellipsoids. Hydrogen atoms, disordered *tert*-butyl groups, and a free PF₆⁻ anion were omitted for clarity.

Table S6 Selected bond lengths (Å) and angles (deg) for **6**

Cu-N	2.097(3)	N-Cu-F1	144.32(9)
Cu-P1	2.2613(10)	N-Cu-P1	82.90(8)
Cu-P2	2.2638(9)	N-Cu-P2	83.39(8)
Cu-F1	2.241(2)	P1-Cu-P2	157.34(4)
P3-F1	1.637(2)	Cu-F1-P3	128.95(13)
P3-F2	1.586(2)	P1-Cu-F1	102.98(6)
P3-F3	1.588(2)	P2-Cu-F1	98.69(6)
P-F of free PF ₆ ⁻ (av.)	1.576(3)		

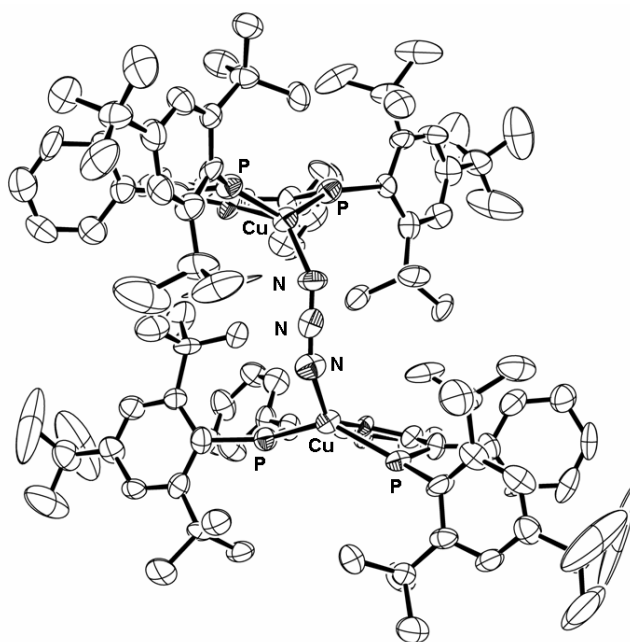


Fig. S6 ORTEP drawing of **7a** with 50% probability ellipsoids. Hydrogen atoms and a free SbF_6^- anion were omitted for clarity.

Computational Details. Geometries optimization, energy, and NAO analysis were performed with DFT method, where the B3LYP functional was used. Optimization was performed with C_2 symmetry in the structures. Full optimization without any structural constraints resulted in $\mathbf{6}^{\text{FREE}}$. This structure exhibited one small imaginary frequency (-15.86 i cm^{-1}), which breaks C_2 symmetry of the molecule (Figure S9). The optimized geometry of $\mathbf{6}'$, in which the geometry of Cu-PF₆-Cu core was fixed, exhibits four imaginary frequencies as a result of constraints (Figure S8). The structural optimization and NBO analysis employed the triple- ζ SDD basis set for copper, 6-31G(d) for P, N and F,⁴ and 6-31G for C and H. Core electrons of Cu (up to 2p) were replaced with effective core potentials (ECPs).⁵ The Gaussian 03 program package was used for all calculations.⁶ Molecular orbitals were drawn with the GaussView 5.0 program package.

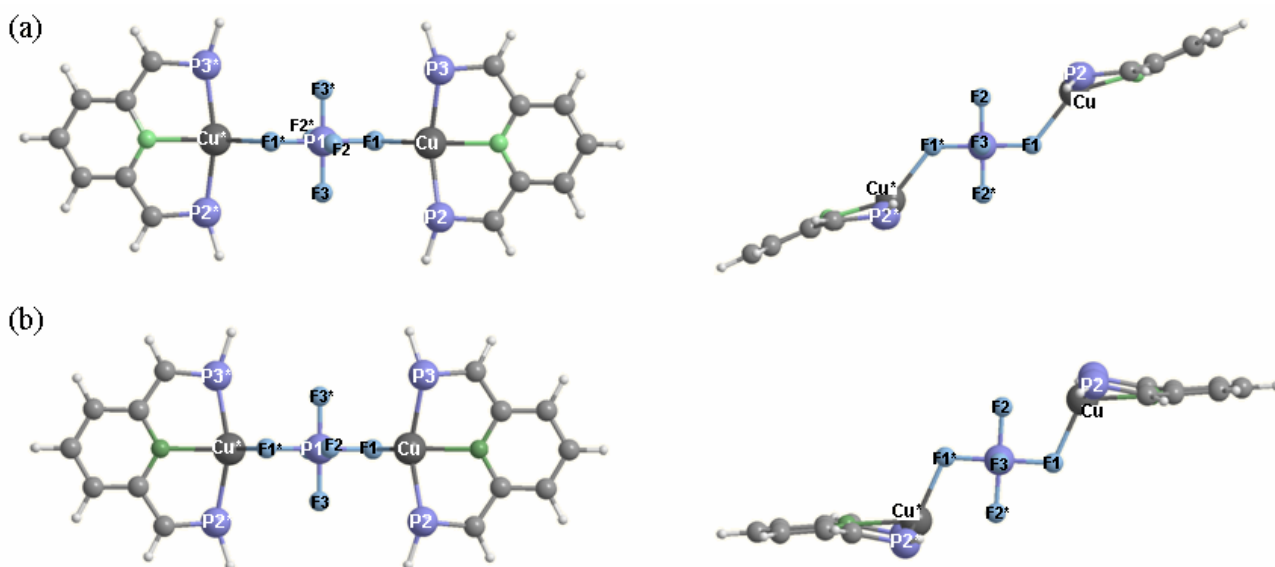


Fig. S7 Optimized geometry of $\mathbf{6}'$ (a) and $\mathbf{6}^{\text{FREE}}$ (b)

Table S7 Selected bond lengths and angles of **6'** and **6'^{FREE}**

	6'	6'^{FREE}	6 (X-ray)
Cu-P2	2.34	2.36	2.2613(10)
Cu-P3	2.34	2.36	2.2638(9)
Cu-N	2.12	2.14	2.097(3)
Cu-F1	2.24	2.16	2.241(2)
Cu-F2	3.05	2.48	3.054
P1-F1	1.64	1.67	1.637(2)
P1-F2	1.59	1.64	1.586(2)
P1-F3	1.59	1.62	1.588(2)
P2-Cu-P3	153.6	147.2	157.34(4)
N-Cu-F1	144.3	117.7	144.32(9)
Cu-F1-P1	129.0	111.45	128.95(13)

Table S8 Absolute total energies (in Hartree) of **6'** and **6'^{FREE}**

	6'	6'^{FREE}
Total energy	-3351.777350	-3351.792734

Table S9 Natural charge by NBO analysis

	6'	6'^{FREE}	[Cu(BPEP)]⁺	PF₆⁻
Cu	0.78	0.79	0.67	
P2,3	0.36	0.36	0.36	
N	-0.54	-0.54	-0.54	
P1	2.78	2.74		2.65
F1	-0.61	-0.60		-0.61
F2	-0.60	-0.59		-0.61
F3	-0.60	-0.59		-0.61
Total charge of PF ₆	-0.84	-0.82		-1.00

Table S10 Mayer's bond order

	6'	6'^{FREE}
Cu-F1	0.32	0.32
Cu-F2	0.13	0.23
Cu-F3	0.03	0.04
P1-F1	0.66	0.65
P1-F2	0.82	0.74
P1-F3	0.87	0.85

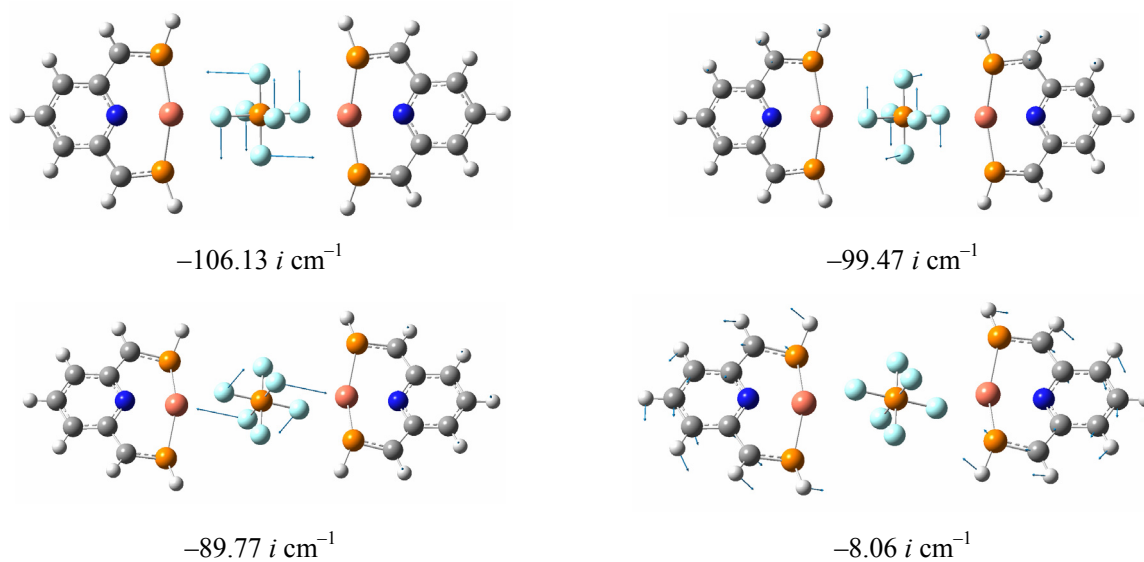


Fig. S8 Imaginary frequency of $6'$

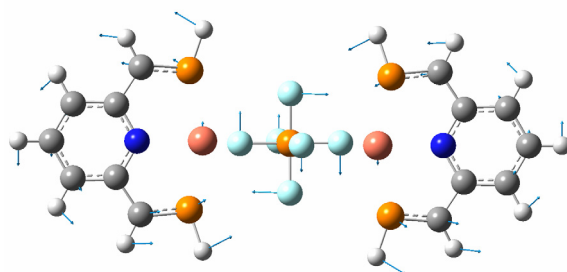
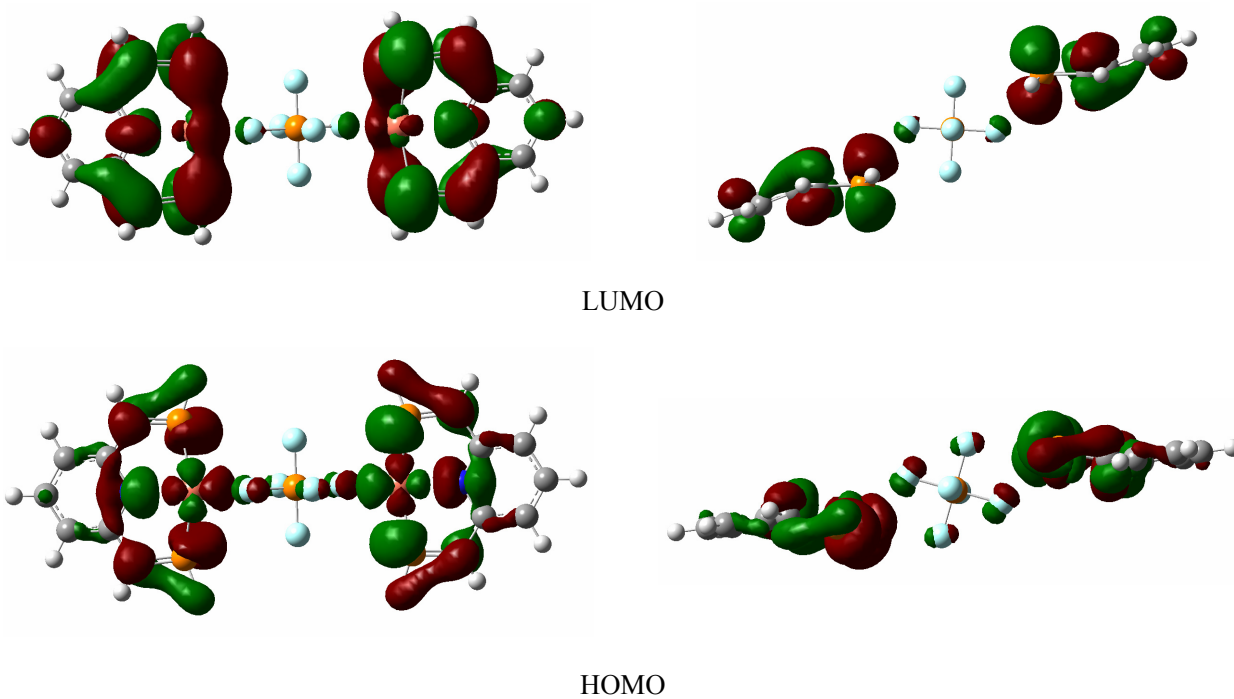


Fig. S9 Imaginary frequency of $6'^{\text{FREE}}$ ($-15.86 i \text{ cm}^{-1}$)



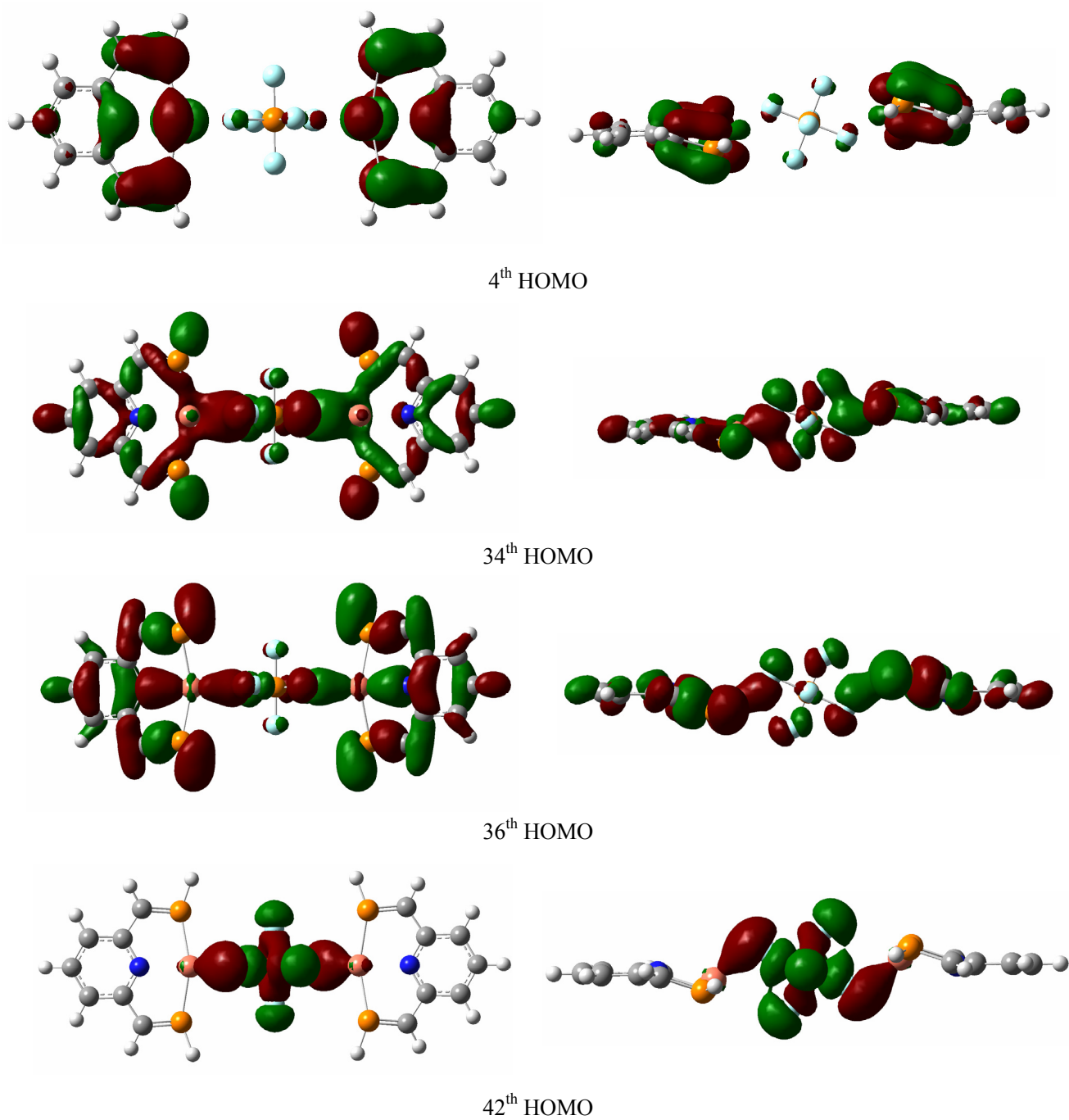


Fig. S10 Selected Kohn-sham orbitals of **6'** including orbital overlaps between Cu and PF_6

Table S11 Cartesian coordinates of **6**⁺

P	0.000000	0.000000	0.000000
F	0.000000	0.000000	1.640000
F	1.590000	0.000000	0.000000
F	0.000000	1.590000	0.000000
F	0.000000	0.000000	-1.640000
F	-1.590000	0.000000	0.000000
F	0.000000	-1.590000	0.000000
Cu	1.739060	0.000000	3.048897
P	2.238967	2.280067	3.237080
P	2.238967	-2.280067	3.237080
N	2.296990	0.000000	5.091468
C	2.621155	1.179326	5.691669
C	3.196411	1.203392	6.976677
H	3.418398	2.153568	7.447697
C	3.432513	0.000000	7.642807
H	3.871474	0.000000	8.633734
C	2.621122	-1.178647	5.691885
C	3.141857	-1.205482	6.999884
H	3.364708	-2.155694	7.470192
C	2.383043	2.396430	4.918213
H	2.364372	3.338599	5.457994
C	2.383166	-2.396051	4.918852
H	2.364561	-3.338029	5.458969
H	1.862323	3.601890	2.889519
H	1.862323	-3.601890	2.889519
Cu	-1.739060	0.000000	-3.048897
P	-2.238967	2.280067	-3.237080
P	-2.238967	-2.280067	-3.237080
N	-2.296990	0.000000	-5.091468
C	-2.621155	1.179326	-5.691669
C	-3.196411	1.203392	-6.976677
H	-3.418398	2.153568	-7.447697
C	-3.432513	0.000000	-7.642807
H	-3.871474	0.000000	-8.633734
C	-2.621122	-1.178647	-5.691885
C	-3.141857	-1.205482	-6.999884
H	-3.364708	-2.155694	-7.470192
C	-2.383043	2.396430	-4.918213
H	-2.364372	3.338599	-5.457994
C	-2.383166	-2.396051	-4.918852
H	-2.364561	-3.338029	-5.458969
H	-1.862323	3.601890	-2.889519
H	-1.862323	-3.601890	-2.889519

Table S12 Cartesian coordinates of **6**^{FREE}

Cu	0.037917	-0.001670	0.085104
P	-0.564390	-2.263293	0.361203
P	-0.566588	2.257370	0.374274
N	-1.787564	0.000822	-1.033471
C	-2.396860	-1.176978	-1.330855
C	-3.608991	-1.203083	-2.048034
H	-4.064329	-2.153008	-2.301563
C	-4.209987	0.002544	-2.414893
H	-5.138198	0.003274	-2.974523
C	-2.400069	1.178958	-1.321861
C	-3.612912	1.207277	-2.037841
H	-4.071263	2.157803	-2.283488
C	-1.740001	-2.389965	-0.849751

H	-2.075807	-3.338121	-1.258901
C	-1.746186	2.390307	-0.832034
H	-2.085765	3.340722	-1.232814
H	-0.093643	-3.600235	0.421082
H	-0.102089	3.595870	0.447174
P	3.217700	-0.001306	0.000000
F	1.894186	-0.001592	-1.023535
F	4.227054	-0.001551	-1.291402
F	3.217700	1.614207	0.000000
F	4.541214	-0.001592	1.023535
F	2.208346	-0.001551	1.291402
F	3.217700	-1.616874	0.000000
Cu	6.397483	-0.001670	-0.085104
P	6.999790	-2.263293	-0.361203
P	7.001988	2.257370	-0.374274
N	8.222964	0.000822	1.033471
C	8.832260	-1.176978	1.330855
C	10.044391	-1.203083	2.048034
H	10.499729	-2.153008	2.301563
C	10.645387	0.002544	2.414893
H	11.573598	0.003274	2.974523
C	8.835469	1.178958	1.321861
C	10.048312	1.207277	2.037841
H	10.506663	2.157803	2.283488
C	8.175401	-2.389965	0.849751
H	8.511207	-3.338121	1.258901
C	8.181586	2.390307	0.832034
H	8.521165	3.340722	1.232814
H	6.529043	-3.600235	-0.421082
H	6.537489	3.595870	-0.447174

Table S13 Cartesian coordinates of [Cu(BPEP)]⁺

Cu	-0.007308	0.000000	-0.002939
N	-0.473911	0.000000	-2.137886
P	-0.087562	2.254069	-0.325316
P	-0.087562	-2.254069	-0.325316
C	-0.621106	1.176528	-2.785019
C	-0.621106	-1.176528	-2.785019
C	-0.440336	2.387385	-1.968468
C	-0.930595	1.209544	-4.157927
C	-0.440336	-2.387385	-1.968468
C	-0.930595	-1.209544	-4.157927
C	-1.085002	0.000000	-4.842874
H	-0.546157	3.346989	-2.466279
H	-0.546157	-3.346989	-2.466279
H	0.017362	3.589959	0.118147
H	0.017362	-3.589959	0.118147
H	-1.046625	2.157685	-4.669086
H	-1.046625	-2.157685	-4.669086
H	-1.324143	0.000000	-5.899856

Table S14 Cartesian coordinates of PF₆⁻

P	15.870677	8.910843	8.878197
F	16.401825	7.758388	7.820516
F	17.035171	8.458359	9.957661
F	14.827407	7.816456	9.545430
F	15.339529	10.063298	9.935878
F	14.706183	9.363326	7.798733
F	16.913948	10.005230	8.210964

References

1. Nakajima, Y.; Nakao, Y.; Sakaki, S.; Tamada, Y.; Ono, T.; Ozawa, F. *J. Am. Chem. Soc.* **2010**, *29*, 9934.
2. Sheldrick, G. M. SHELXS-97; University of Göttingen: Germany, 1997.
3. Sheldrick, G. M. SHELXL-97; University of Göttingen: Germany, 1997.
4. (a) Hariharan, P. C.; Pople, J. A.; *Theor. Chim. Acta* **1973**, *28*, 213. (b) Hariharan, P. C.; Pople, J. A. *Mol. Phys.* **1974**, *27*, 209.
5. Andrae, D.; Haussermann, U.; Dolg, M.; Stoll, H.; Preuss, H. *Theor. Chim. Acta* **1990**, *77*, 123.
6. Frisch, M. J.; Trucks, G. W.; Schlegel, H. B.; Scuseria, G. E.; Robb, M. A.; Cheeseman, J. R.; J. A. Montgomery, J.; Vreven, T.; Kudin, K. N.; Burant, J. C.; Millam, J. M.; Iyengar, S. S.; Tomasi, J.; Barone, V.; Mennucci, B.; Cossi, M.; Scalmani, G.; Rega, N.; Petersson, G. A.; Nakatsuji, H.; Hada, M.; Ehara, M.; Toyota, K.; Fukuda, R.; Hasegawa, J.; Ishida, M.; Nakajima, T.; Honda, Y.; Kitao, O.; Nakai, H.; Klene, M.; Li, X.; Knox, J. E.; Hratchian, H. P.; Cross, J. B.; Adamo, C.; Jaramillo, J.; Gomperts, R.; Stratmann, R. E.; Yazyev, O.; Austin, A. J.; Cammi, R.; Pomelli, C.; Ochterski, J. W.; Ayala, P. Y.; Morokuma, K.; Voth, G. A.; Salvador, P.; Dannenberg, J. J.; Zakrzewski, V. G.; Dapprich, S.; Daniels, A. D.; Strain, M. C.; Farkas, O.; Malick, D. K.; Rabuck, A. D.; Raghavachari, K.; Foresman, J. B.; Ortiz, J. V.; Cui, Q.; Baboul, A. G.; Cliord, S.; Cioslowski, J.; Stefanov, B. B.; Liu, G.; Liashenko, A.; Piskorz, P.; Komaromi, I.; Martin, R. L.; Fox, D. J.; Keith, T.; Al-Laham, M. A.; Peng, C. Y.; Nanayakkara, A.; Challacombe, M.; Gill, P. M. W.; Johnson, B.; Chen, W.; Wong, M. W.; Gonzalez, C.; Pople, J. A. *Gaussian 03 (Revision C.02)*, Gaussian, Inc., Wallingford CT 2004.